Research Article GU J Sci, Part A, 12(1): 228-249 (2025) 10.54287/gujsa.1589209

Gazi University
Journal of Science
PART A: ENGINEERING AND INNOVATION
http://dergipark.org.tr/gujsa

Mineral Chemistry of Ulukale Porphyritic Dome and Çağlarca Radial Dykes in the Tunceli Volcanites, Eastern Turkey

Sevcan KÜRÜM[1*] Abdullah SAR[1] Muhammed Yasir YURT[1]

[1] *Fırat University, Faculty of Engineering, Department of Geological, 23119, Elazığ, Türkiye*

Keywords

Tunceli Volcanics
Ulukale-Çağlarca
Porphyritic Dome
Radial Dyke
Mineral Chemistry

Abstract

This study presents mineral chemistry data the first time as a analytical data for the Ulukale porphyritic dome and the Çağlarca radial dykes located within the Neogene Tunceli volcanic rocks. In petrographic studies, it was determined that the dome and dykes with porphyritic texture were of trachyandesite composition. Plagioclase (oligoclase + andesine), amphibole (hastingsite + magnesiohastingsite and ferroedenite) and biotite (meroxene + phlogopite) found in domes-dykes, and pyroxene (augite and hypersthene) element contents only in dykes indicate that the magma originated from mantle-mantle+crust mixing and was affected by late-stage low-temperature hydrothermal fluids. Pyroxenes indicating low temperature - pressure conditions also indicate an upper crust source. This magma with mantle + crust properties supports crustal thickening and underplating mafic magma formation, which is a result of the compression regime in the Eastern Anatolia region.

Cite

Kürüm, S., Sar, A., & Yurt, M. Y. (2025). Mineral Chemistry of Ulukale Porphyritic Dome and Çağlarca Radial Dykes in the Tunceli Volcanites, Eastern Turkey. *GU J Sci, Part A, 12*(1), 228-249. doi:10.54287/gujsa.1589209

Author ID (ORCID Number)

0000-0001-6121-5564 Sevcan KÜRÜM
0000-0002-9752-7807 Abdullah SAR
0000-0002-1563-2938 Muhammed Yasir YURT

Article Process

Submission Date 22.11.2024
Revision Date 23.12.2024
Accepted Date 08.01.2025
Published Date 26.03.2025

1. INTRODUCTION

Lava domes and dykes found in volcanic systems are a natural part of the system and are related to many related parameters, as well as the effusive and explosive nature of volcanism (Cassidy et al., 2018). Lava domes, which are products of explosive volcanism, will block the volcano vent and prevent magmatic gas outflow, which will increase the pore pressure and increase the severity of the eruption. For this reason, the eruption intensity of lavas with more acidic composition that constitute explosive volcanism will increase. It is suggested that the effectiveness of gas release is reduced due to the change in the composition of the dome-forming magma by hydrothermal fluids, apart from its viscosity (Ball et al., 2013; Rosas-Carbajal et al., 2016), and therefore the explosion severity is increased (Edmonds et al., 2013; Horwell et al., 2013). In explosive volcanisms, magma flow rate; gas evolution will determine the time available for cooling and crystallization, which will affect the morphology of the dome (Fink & Griffiths, 1998).

In this study, the mineralogical-petrographic and mineral chemistry of the geological structures developed in the form of domes and radial dykes within the Tunceli volcanics, where explosive volcanism is dominant,

*Corresponding Author, e-mail: skurum@firat.edu.tr

and the properties of the magma forming the geological structures were investigated. Since the study was guidet with very local and limited data, it is thought that it will form the basis for future studies.

2. MATERIAL AND METHOD

A large number of thin sections were made in the rocks in the study area and mineral chemistry (major and trace elements) analysis was carried out in a total of five samples, two from dome and three from dykes.

The mineral chemistry analyzes were carried out using Bruker-Axs Quantax XF lash 3001 EDS integrated with a Zeiss Evo-50 EP microscope and JXA 8230 Model device under 20Kv voltage and 15NA current at the laboratories of Ankara University Earth Sciences Application and Research Center (YEBİM (Ankara, Turkey). The preparation and polishing of the thin sections used in these analyzes were carried out in this center. Mineral compositions were determined by converting the major and minor elements of the mineral obtained in oxide form from EPMA (Electron Probe Micro Analysis) into cation values (apfu = atoms per formula unit).

3. GEOLOGICAL BACKGROUND OF EASTERN ANATOLIAN VOLCANISM

The Eastern Anatolia region is considered an active continental plate margin as a result of the final closure of the Neo-Tethys Ocean. In these types of tectonic environments, magmatic activity with very common distribution develops, called orogenic magmatism. This magmatic activity forming linked to continental collision during geodynamic evolution of the region may become much more complicated with the effect of ocean-ocean or ocean-continent convergence (Innocenti et al., 1982; Pearce et al., 1990; Keskin et al., 1998; Turner et al., 2017; Özdemir et al. 2006; Karaoğlu et al., 2016, 2017). Continental collision is defined as the time when two continental plates approaching from opposite directions contact for the first time at the point when oceanic lithosphere or the plate between the two continental plates is fully subducted (Hu et al., 2016). All tectonic, magmatic or metallogenic events controlled by or directed by gravitational imbalance occurring when collision and convergence forces end and features related to probable subduction are defined as post-collisional events (Kuşçu et al., 2007; Xu et al., 2020). This situation can be very clearly observed in the Eastern Anatolian region in terms of both tectonic, magmatic and metallogenic events. Additionally, this situation becomes more complicated with the development of two large transform faults developing after collision and affecting the whole region of the North Anatolian Fault Zone (NAFZ) and East Anatolian Fault Zone (EAFZ) (Figure 1a). With the full development of these two conjugate fault systems, Anatolia began to move as an independent microplate and they are accepted as forming a new triple junction (Eurasia-Arabia-Anatolia) (Agostini et al., 2019).

The Eastern Anatolia region, accepted as one of the best examples of a continental collision belt in the world, is considered to still be actively deformed as a result of north-south compression (Keskin, 2005). Accepted as beginning in the Late Oligocene from the initiation of the continental collision (Arabia-Eurasia) in Eastern Anatolia, magmatism forms the East Anatolia Magmatic Belt with distribution toward the east (Rabayrol et

al., 2019) (Figure1a, 1b). The earliest magmatic phase in this belt is the Cevizlidere magmatism with 26-25 Ma (Oligocene) (İmer et al., 2015), then this magmatism increased over time and formed the largest volume Erzurum-Kars volcanic plateau in the Late Miocene (11.6-5.3 Ma). The volcanism forming the Erzurum-Kars volcanic plateau developed in three different stages and the first stage (11-6 Ma) was stated to involve basic volcanism from small temporary chambers, while acidic volcanism erupted from large, zoned magma chambers (Keskin et al., 1998) (Figure 1a). Researchers stated that volcanism in the middle stage (mostly between 6-5 Ma) was characterized by single-stage volcanism forming dominantly from andesitic-dacitic lavas and later due to crystallization of aqueous assemblages (containing amphibole) in deeper magma chambers. Late stage volcanism (mostly 5-2.7 Ma) was stated to be characterized by bimodal volcanism comprising basically plateau basalts and basaltic andesite lavas and felsic domes (Keskin et al., 1998). The main magma forming this volcanism on the plateau was affected by subduction events before collision and is accepted as having the features of lithospheric-derived magma carrying traces of subduction.

The Mazgirt (Tunceli) volcanics of Early-Middle Miocene (16.3 and 15.1 Ma), which are among the Tunceli volcanics and reflect the geodynamic framework of the Eastern Anatolia region, represent arc volcanism due to the Eurasia-Arabia convergence. The Late Miocene Tunceli basalts (11.4-11.0 Ma) are accepted as the beginning of post-collisional tectonics in Eastern Anatolia, while the Karakoçan (4.1 Ma) and Elazığ volcanic rocks (1.9-1.6 Ma) are accepted as being emplaced after the initiation of strike-slip movement on the North Anatolian and East Anatolian fault systems (Agostini et al., 2019) (Figure 1b).

Many studies were performed related to regional magmatism for all these reasons (Arger et al., 2000; Kürüm et al., 2008; Önal et al., 2008; Karslı et al., 2008; Kaygusuz, 2009; Lebedev et al., 2016; Karaoğlu et al., 2020; Oyan et al., 2016; Kaygusuz et al., 2018; Rabayrol et al., 2019; Kürüm & Baykara, 2020). Magmatism beginning from the initiation of Arabian plate collision in the Late Oligocene and defined as Late Cenozoic magmatism in Eastern Anatolia displays a variation in character from alkaline (hawaiite, mugearite) (Oyan et al., 2017) to calcalkaline and weak tholeiitic characteristics linked to geographical, sedimentological and tectonic variations.

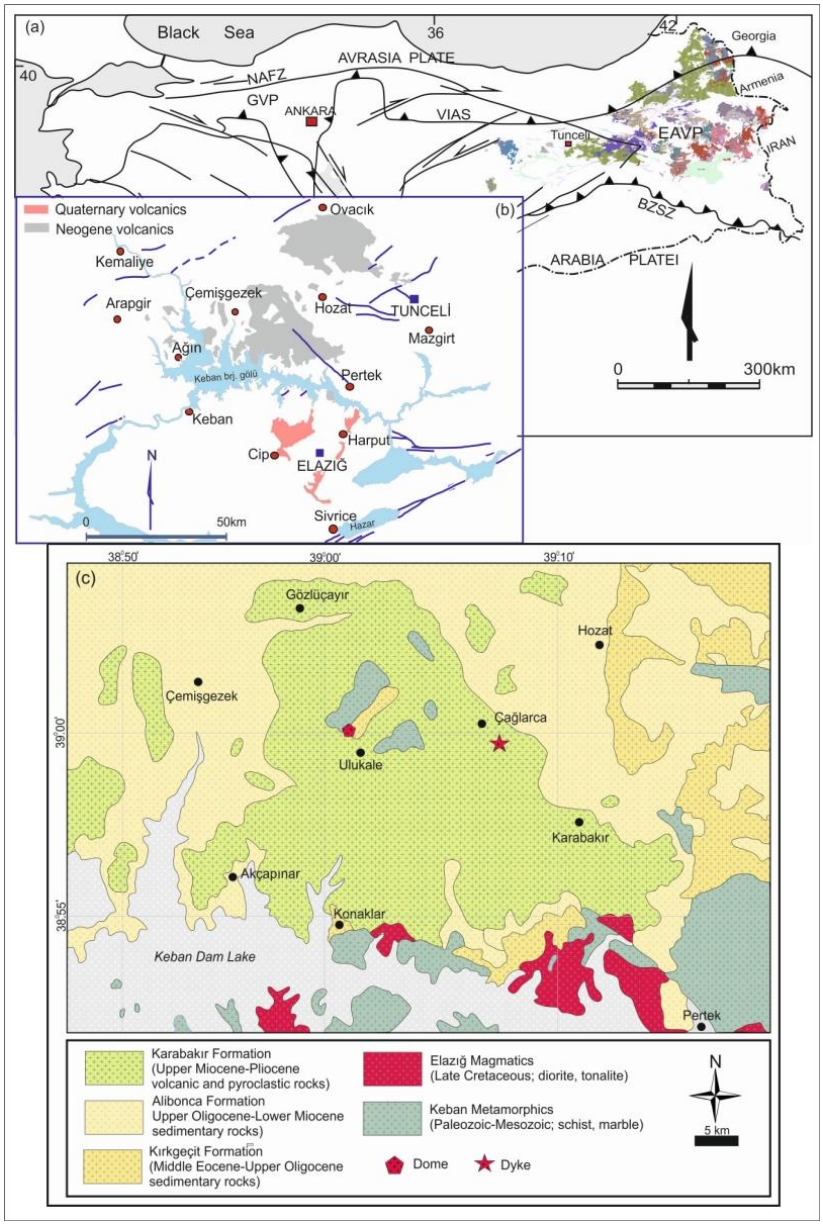

Figure 1. a) *View of the simplified tectonic units of Turkey and post-collision spreading volcanism in Eastern Anatolia (East Anatolian Volcanic Province) (MTA, 2002),* ***b)*** *View of the spreading volcanism in Tunceli and Elazığ area, and location map of the study area,* ***c)*** *Simplified geological map of the Ulukale and Çağlarca around (redrawn from Geological Map of Turkey, 1:500.000, Sivas sheet) (from Kürüm et al., 2024). EAVP: East Anatolian Volcanic Province, GVP: Galatean Volcanic Province, VIAS: Vardar-Izmir-Ankara Suture Zone, NAFZ: North Anatolian Fault Zone, BZSZ: Bitlis Zagros Süture Zone.*

Volcanism in the region appears to have variable composition and eruptive forms linked to compositional changes in the magma. For example, there are both Ocean Island Basalt (OIB)-type lavas with basic composition (Aydın et al., 2014; Kürkçüoğlu et al., 2015; Lustrino et al., 2010; Lebedev et al., 2016) and volcanics derived from the asthenospheric mantle (sub-slab) that is not affected by pre-collision subduction events (anorogenic volcanic rocks with in-plate geochemical features) (Kocaarslan & Ersoy, 2018). Depending on the different magma source formations, the composition of the volcanism in the region offers lava flow rocks ranging from basic to dacite/rhyolitic composition, as well as a rich pyroclastic sequence that is their equivalent (Pearce et al., 1990; Keskin et al., 1998; Yılmaz et al., 1998; Kürüm & Baykara, 2020). As

a general result of all these studies, a wide variety of models including different source areas, melting regimes and evolution processes have been created. Moreover, it is also stated that, differently, volcanism in Eastern Anatolia occurred by shallow melting of the previously metasomatized Anatolian continental lithosphere mantle and asthenosphere through decompression due to the collision of the Arabian and African asthenospheric mantles (Rabayrol et al., 2019).

4. LOCAL GEOLOGY AND VOLCANO-STRATIGRAPHY

Around Tunceli, there are Keban Metamorphites (Permo-Triassic) consisting of schists and crystallized limestones in the Paleozoic, Munzur Limestones (Jurassic-Cretaceous) and Elazığ Magmatics (Upper Cretaceous) in the Mesozoic, while in the Cenozoic; Eocene Kırkgeçit Formation in the turbiditic flysch facies, Oligo-Miocene Alibonca Formation and Miocene volcanics (Tunceli Volcanics/Karabakır Formation) crop out (Figure 1c). Of these units, only the Permo Triassic Keban Metamorphics form a contact with the Ulukale dome in the study area (Figure 1b). The Upper Cretaceous Elazığ Magmatic rocks basically comprise diorite group rocks (quartz diorite, diorite, monzodiorite and quartz monzodiorite) with granite, tonalite, quartz monzonite and gabbro (Kürüm et al., 2011; Sar et al., 2022). Dating studies for different lithologies determined the age of the unit varied from 59.77 ± 1.2 - 84.35 ± 1.7 Ma (Kürüm, 2011; Lin et al., 2015; Beyarslan & Bingöl, 2018; Sar et al., 2019). The Middle Eocene-Upper Oligocene Kırkgeçit Formation is found above the Elazığ Magmatic rocks in the south of the study region and are generally layered. The Upper Oligocene-Lower Miocene Alibonca Formation forms the boundary with the studied volcanic rocks. Volcanic rocks contacting metamorphics around Ulukale village have angular unconformity with the Alibonca Formation near Çemişgezek and with the Alibonca and Kırkgeçit Formations and Elazığ Magmatics to the south (Figure1c).

Volcanism in the study area and close surroundings mainly formed explosive/extrusive volcanism products with a very thick sequence. These volcanic products, described as pyroclastic rocks, begin with tuffs above the Elazığ Magmatic rocks, Kırkgeçit and Alibonca Formation forming the basement around Çemişgezek in the west and in the south. Tuffs, occasionally forming very thick sequences, are basically not well consolidated and as a result of not being resistant to surface conditions, they form generally soft topography with ridges, with very severe erosion especially in river beds. In the field, weathered surfaces appear to be dirty white and gray in color.

Contrary to the common tuffs in the region, generally volcanic breccia forms the thickest sequence within pyroclastics. Found very widely, volcanic breccia formed of pebbles and blocks comprising many different grain sizes and shapes (from a few cm to m) contain occasional pumice levels and occasional lava layers locally or in pockets. Sometimes small-scale andesitic porphyry is observed to have intruded into tuff. Generally, the volcanic breccia comprise angular pebbles and blocks with different sizes and compositions, with nearly all pebble and block size grains having volcanic origin and being heterogeneous. This pyroclastic rocks appears to be the most important factor forming the current morphological structure of the region.

They reach thickest levels especially in the south close to the area containing dykes, on the south slopes of Akdemir (Şavak) village and south of Ulukale dome (Figure 2a, 2b). The rocks formed by the lava at the top of this thick sequence have not been eroded, so a very rugged and differently shaped terrain was formed due to erosion of less resistant pyroclastics (Figure 2b). Contrary to this, volcanism (lava rocks and pyroclastics) further west in the study area (W of Çemişgezek) generally form soft/smooth topography. Pyroclastic products in the region generally have tuff lithology. While lava flow rocks in the region have more basic composition and are more common in the west near Çemişgezek, the study area and surroundings have features of more acidic-intermediate composition.

The lava dome, which is the subject of the study, is thought to be the last product of volcanism in the region (Kürüm et al., 2024). This geological structure, which has an altitude of approximately 300m and a spreading area of 4.80km, is massive and differs from the surrounding pyroclastic and other volcanic rocks due to its very hard and crack-free feature (Figure 2a). It is expected that uplift-tilt and differentiation zones will be observed in the contact zones of the porphyritic dome, which is the final emplacement product of this type, with pyroclastics. Traces of dome formation are not observed in the surrounding rocks, probably due to high erosion. This dome, in which porphyritic texture is clearly observed, is thought to have formed sub-volcanically near the surface.

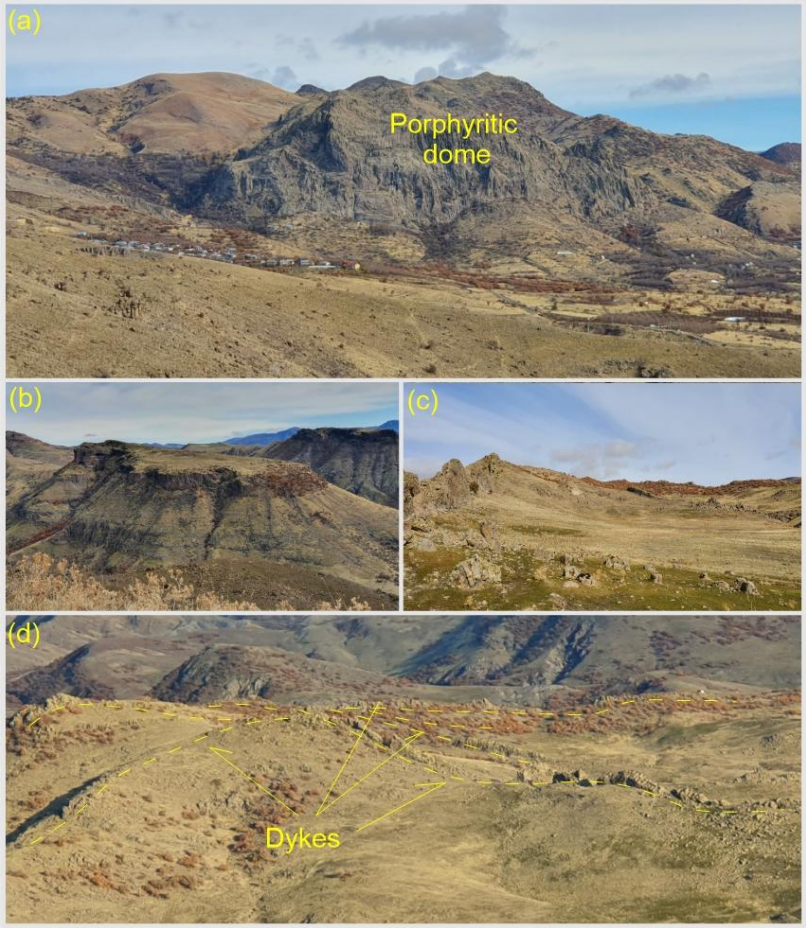

Figure 2. *The view of the* ***a) b)*** *Ulukale porphyritic dome and* ***c) d)*** *Çağlarca radial dykes*

The radial dykes, which constitute the subject of the study, extend in different directions from a central exit point, again within the pyroclastics and in accordance with theoretical definitions. Radial dykes, which were formed by settling in the fractures that reached the surface during the period when the volatile component of the magma decreased, are found in pyroclastic rocks. Seven dykes were identified from the same center in different directions and forming a radial shape (Figure 2c, 2d). Although the length and height of the dykes vary, their thickness is approximately similar. Generally, a very dense crack system is observed in all dykes. It is more altered and weaker than dome rock samples. The weathered surfaces of rocks with porphyritic texture generally appear in grayish colors. One of the longest dykes, the 3rd dyke from the left, is in the 20^0SW direction from the exit center to the road and is approximately 1400 m long and is important because it creates a height of 10 m in places. This dyke changes direction 30° to the east approximately 150 m from the beginning (Figure 2d). The other important dyke in the region, the 6th dyke from the leftmost dyke, is in the 10^0SE direction from the center of the outlet and is 1500 m long. The 4th and 5th dykes, which developed in approximately the same direction (20SW), are 360m and 550m long, respectively. The other two dykes extend towards the W and are relatively shorter.

Erciyes Volcano/volcanism (Holocene), which is one of the volcanoes showing a dome structure in the Central Anatolia Region, located further west of the study area, is a stratovolcano volcanism in which the products of different eruption types can be seen together. After the Koçdağ caldera, which is a large caldera, developed on the Erciyes Stratovolcano, many dome and cinder cones developed along the radial faults around the volcano. Domes are mostly acidic and medium in composition. Although the domes in the Erciyes volcanism are similar in composition to the Ulukale dome, they are different in terms of formation mechanism. Again, within the Central Anatolian volcanics, the Göllüdağ volcanism is composed of rhyolitic pyroclastics, dome settlements and lava flows. In Göllüdağ volcanism, post-caldera activities after caldera formation are manifested by local rhyolitic dome outflows (Atıcı & Türkecan, 2017).

5. DISCUSSION

5.1. Petrography

The rocks formed by lavas from the Ulukale porphyritic dome have a micro-porphyritic texture and consist mainly of plagioclase, biotite, amphibole, sanidine and quartz. Plagioclases are found as phenocrystals and microliths, and comprise the main phenocrystal phase in the rock (Fig 3a, 3b). Plagioclase phenocrysts occasionally contain dissolution structures and small prismatic plagioclase laths, indicating magma mixing (Hibbard, 1991). Biotites are the mineral most commonly found after plagioclase (Figure 3b-3d). Amphiboles are found as prismatic or hexagonal crystals (Figure 3d), sanidine crystals have Carlsbad twinning, while quartz are anhedral. Generally minerals in the rocks have low-moderate levels of alteration. The abundances of minerals found as phenocrystals in the rock; plagioclase > biotite > amphibole > sanidine > quartz. All these minerals also constitute the microcrystalline material of these porphyritic textured rocks. Some plagioclase minerals in the rock generally have alteration observed as seritization and clay mineral

formation, while oxidization or chloritization is clearly observed in the groundmass. Based on all these general textural and mineralogical features, the Ulukale porphyritic dome may be said to have trachyandesite composition.

The Çağlarca radial dykes are found with different lengths and different strikes from a center in the study area. Samples from these dykes have similar textural features to the Ulukale dome. The main mineral composition of the dykes comprises plagioclase, amphibole and biotite, in order of abundance, with lower rates for sanidine and quartz. Plagioclases are generally prismatic euhedral-subhedral crystals, polysynthetic and with albite twins and occasional zoned structure (Figure 3e). In dyke samples, different to dome samples, the most abundant mineral after plagioclase is amphibole (Figure 3e, 3f). Amphiboles, found at high rates within groundmass, are generally small crystals with euhedral-anhedral form. Biotite minerals found in dykes occasionally have bladed form indicating magma mixing, while they occasionally contain plagioclase and amphibole mineral inclusions. Sanidine phenocrystals have Carlsbad twinning. Alteration observed in the rock in generally is seen in sanidines. Dykes with porphyritic textural features contain groundmass comprising microcrystalline forms of all minerals in the rock. Alteration in the rock in general is occasionally intensely observed in the groundmass, which appears to have dark color and be oxidized. The Çağlarca dykes have trachyandesite composition.

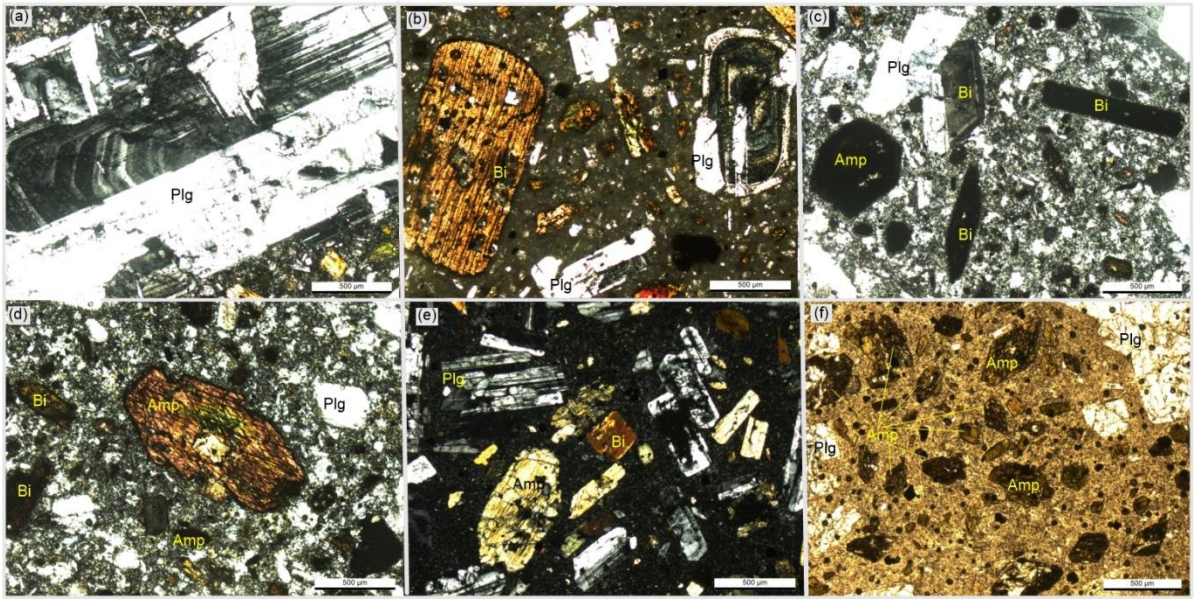

Figure 3. *Representative photo micrographs of texture and mineral assemblages in the* ***a) b) c) d)*** *Ulukale porphiritic dome and* ***e) f)*** *Çağlarca radial dykes. Plg; Plagioclase, Amp; Amphibole, Bi; Biotite (****a-e****; cross-polarized light,* ***f****; plane-polarized light)*

5.2. Mineral Chemistry

Analyses were performed on plagioclase, biotite, amphibole and pyroxene minerals identified in a total of five samples, two from the Ulukale porphyritic dome (Y1, Y5) and three from the Çağlarca radial dykes (Y6, Y9, Y11).

5.2.1. Plagioclase

Six different plagioclase minerals from two samples belonging to Ulukale porphyritic dome (Y1-Y5) were analyzed at a total of 37 points (Supplementary Table 1). Measurements in samples from the dome found the content of anorthite, orthoclase and albite varied from An_{38-22}, Or_{6-2}, Ab_{74-60}. According to these results, feldspars from porphyritic dome samples appear to have oligoclase and andesine composition (Figure 4).

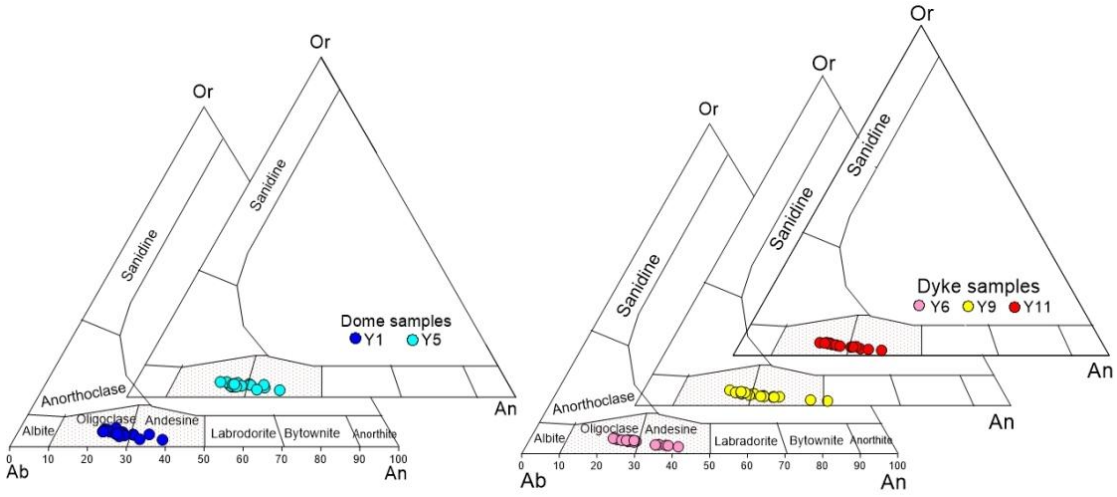

Figure 4. *Composition of plagioclase in the classical An-Ab-Or scheme (Deer et al., 1992) for Ulukale dome and Çağlarca radial dykes*

Ten different plagioclase minerals from three samples (Y6, Y9, Y11) from the dykes were analyzed at a total of 51 points (Supplementary Table 1). According to the analysis results, dyke samples had anorthite, orthoclase and albite contents varying in the interval An_{46-22}, Or_{5-1}, Ab_{75-48}. Based on these results, dykes appear to have similar plagioclase composition as samples from the dome. However, differently, plagioclase in the dykes had near equal rates of andesine-oligoclase composition and also had labradorite composition, though at low rates (Figure 4).

To determine the relationships between elements in plagioclase minerals, a binary variation graph of Na (apfu), Al (apfu), Ca (apfu) and K (apfu) versus Si (apfu) was drawn (Figure 5). All examples show similar trends, consistent with each other. This distribution of elements indicates fractionation.

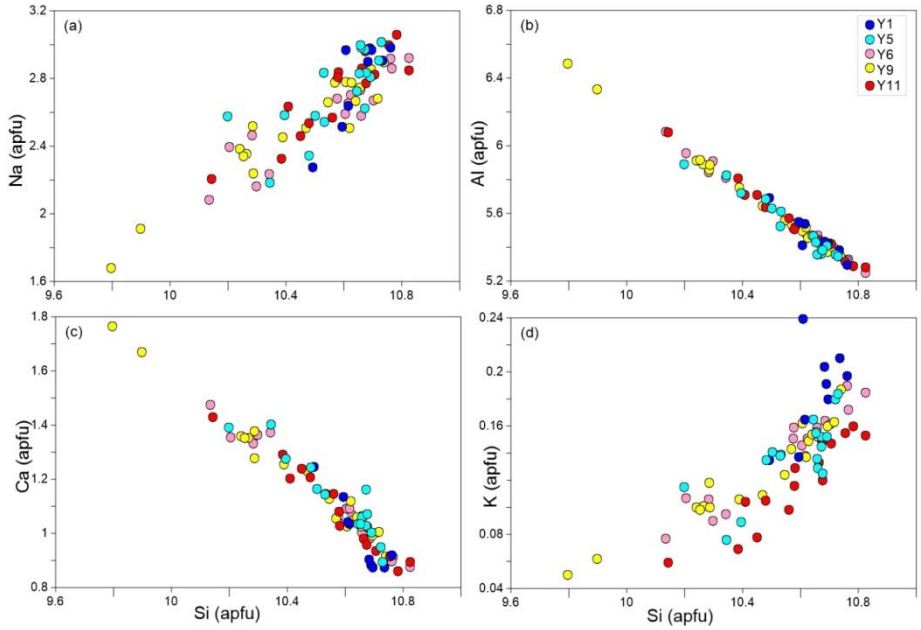

Figure 5. *Change diagrams of elements according to Si (apfu) in plagioclase minerals*

5.2.2. Pyroxene

Pyroxene mineral was detected only in dykes. In samples numbered Y9 and Y11, a total of 12 points were analyzed for 3 different pyroxene minerals. According to the analysis results calculations, the Mg# of samples Y9 and Y11 vary between 0.76-0.82- 0.73-1.12 respectively (Supplementary Table 2). To see the compositional changes of pyroxenes, binary graphs of element (cation, apfu) contents versus Mg# were drawn (Figure 6). Except for the two analysis points with the highest Mg# in the Figure 6, the other analyzes are generally compatible with each other. At these two samples Si, Ca, Na is at the lowest value and Ti, Al, Fe, K is at the highest value compared to the other points (Figure 6). This compositional difference may indicate that different thermodynamic conditions developed during crystallization. According to the $Mg_2Si_2O_6$ (Enstatite) - $Ca_2Si_2O_6$ (Wollastonite) - $Fe_2Si_2O_6$ (Ferrosillite) values calculated from the main element contents of pyroxenes, the pyroxene in radial dykes generally had augite composition. However, only two sample amount with hyperstene composition was identified (Figure 7a). It is accepted that especially Al and Ti elements in pyroxenes limit the pressure conditions in which the mineral crystallizes (Nekvasil et al., 2004). For this purpose, the diagram developed and calibrated from experiments on terrestrial alkaline basalts shows the pressure dependence of the Al-Ti ratio for pyroxenes in equilibrium with basaltic magma (Nekvasil et al., 2004). Pyroxenes crystallizing from magma with basic composition must have high Al-Ti ratios since they are formed under high pressure conditions. Accordingly, it is seen that the examined samples have a very low Al-Ti ratio (except for two samples with hypersthene composition) in the Al-Ti diagram (Figure 7b), therefore the pyroxenes in volcanics crystallize without any difference under low pressure conditions. Similarly, in Figure 7c and 7d, it can be seen that pyroxenes represent low-pressure conditions. In Figure 7c, despite the low Ca+Na content of the samples, the relatively higher Ti content indicates calc-alkaline basalt source which is also consistent with the geochemical data (Kürüm et al., 2024).

According to Al content, pyroxenes give the composition of crustal basalt (Figure 7d) and this also indicates equilibrium crystallization.

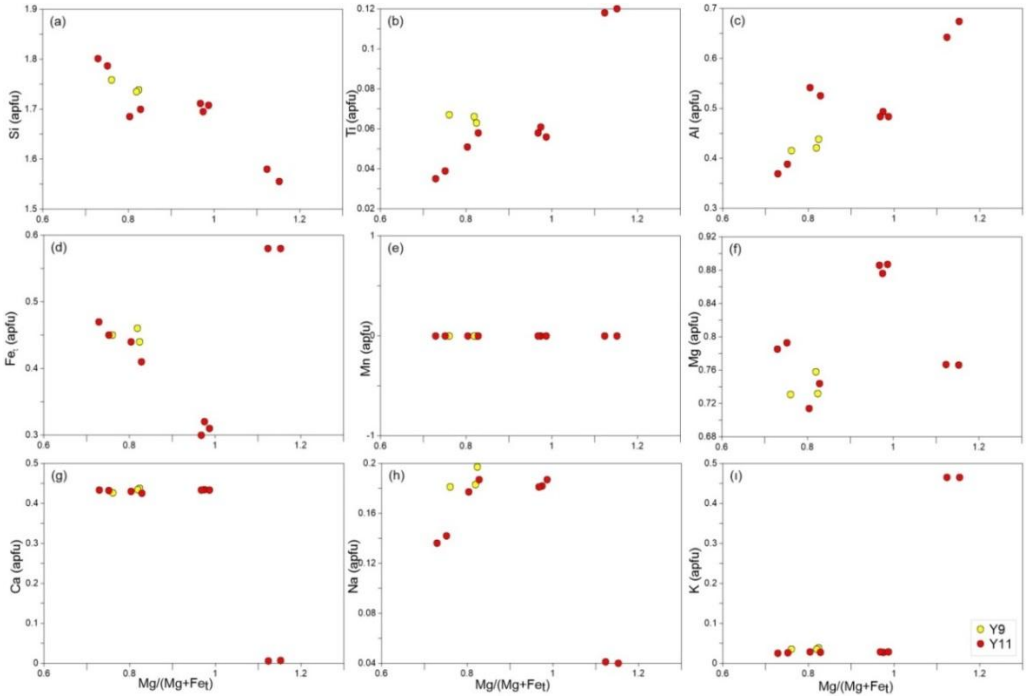

Figure 6. *Binary variation diagrams for the main element compositions of pyroxenes*

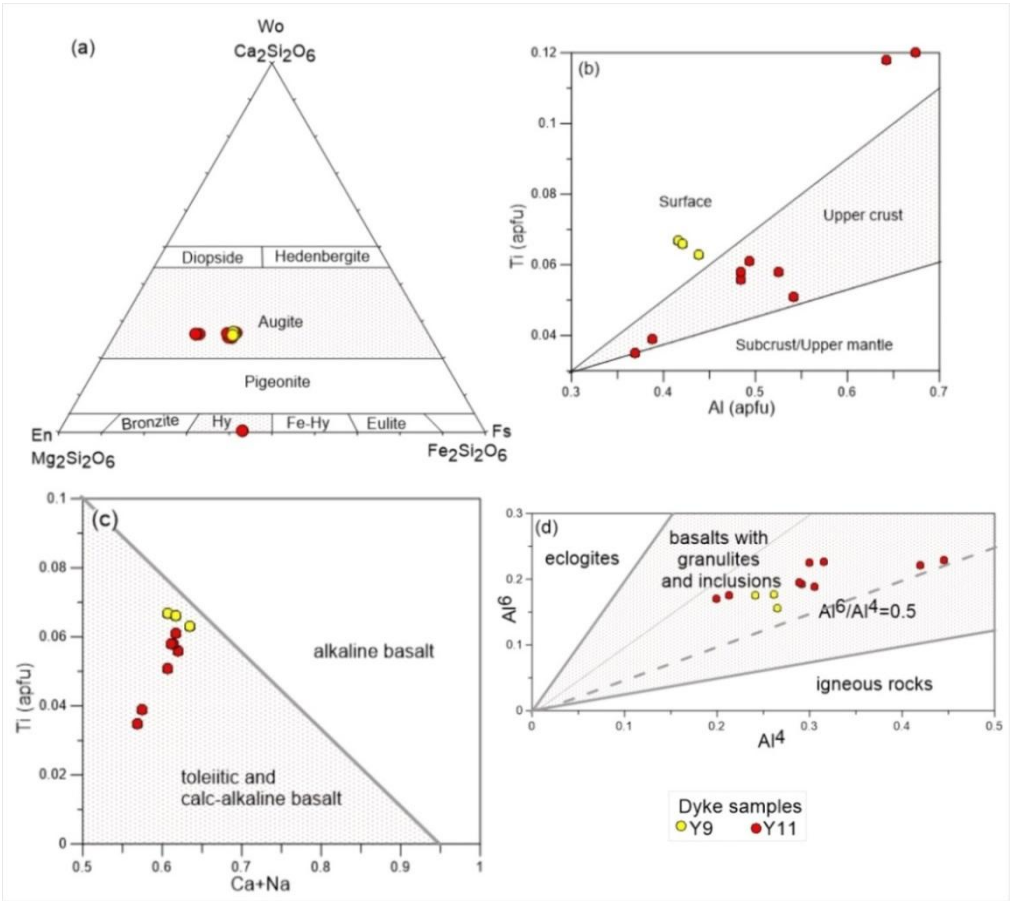

Figure 7. *Classification and discriminant diagrams for pyroxene of volcanics that are the subject of the study.* ***a)*** *En–Wo–Fs diagram (Morimoto et al., 1988),* ***b)*** *Crystallization depth model according to Al-Ti*

contents (Nekvasil et al., 2004), ***c)*** *Ti vs (Ca+Na) diagram (Leterrier et al., 1982),* ***d)*** *Al^6 vs Al^4 (Aydın et al., 2009)*

5.2.3. Amphibole

From the studied rocks, one sample from the porphyritic dome (Y1) and three samples (Y6, Y9, Y11) from the dykes had amphibole mineral chemistry analysis performed. A total of 14 points in 3 different minerals in the sample from the dome were analyzed. A total of 59 points were analyzed in 10 different amphibole minerals from the dykes, with three minerals from sample Y6, four minerals from sample Y9 and three minerals from sample Y11. Analysis data and calculations from all samples are given in Supplementary Table 3. The Si value of the Ulukale porphyritic dome amphibole samples is 5.60-6.58 apfu, except for one sample, and the Si value of the dykes is the same as the Si 5.86-6.58 apfu. Although the Mg values of domes and dykes, varying between 0.55-0.74% and 0.60-0.75%, are similar, and especially Ca (0.00-1.63; 1.67-1.86) values are different. According to Si and Mg# values, it is seen that amphiboles are mainly composed of hastingsite and magnesiohastingsite (Figure 8a). A smaller number of samples also have ferrodenite composition.

Additionally, it is seen that their amphiboles do not exceed the values of Si = 7,500 (apfu), which represents the silica content limit of magmatic amphiboles according to Leake (1971) (Figure 8b). The identification of all samples as magmatic amphiboles indicates that metasomatism is not effective in these amphiboles.

In experimental studies, it has been determined that oxygen fugacity exerts a dominant control on the Fe/(Fe+Mg) ratio of mafic silicates (Zhang et al., 2015; references in the paper). Created for this purpose, the Al^{IV} vs. Fe/(Fe+Mg) diagram (Anderson & Smith,1995), it can be said that the amphiboles of the rocks under study were formed under very different - high and low - oxygen fugacity conditions (Figure 8c). All amphibole samples show the same feature. In the TiO_2 and Al_2O_3 diagram (Jiang & An, 1984) created based on amphibole main oxide data used to distinguish magma sources, a few dyke samples reflect the mantle-crust feature, while most of the samples are concentrated in the mantle source region (Figure 8d). The dome samples are located entirely in the mantle region. Samples indicating mantle origin according to Al_2O_3 content indicate mantle+crust mixing source according to MgO content. This can be considered as a sign of mafic magma settling/mixing in the felsic magma chamber in the crust.

5.2.4. Biotite

Biotites are common ferromagnesian silicate minerals in the rocks under study where it occurs as an early- to late-stage crystallization mineral. Total of 6-18 different points had biotite mineral chemistry analysis performed in 11 different biotite minerals obtained from 5 samples (Y1-Y5-Y6-Y9-Y11) from both dome and dykes rocks (Supplementary Table 4). The biotites in dome and dykes show variation in SiO_2 content from 45.5-34.6 and 36.9-32.9 wt% respectively. Dyke biotite samples had total Al content from 2.8-2.5% atoms per formula unit (apfu), with this ratio varying from 2.7-2.5% apfu in Ulukale porphyritic dome

samples. The $Fe^{2+}/(Fe^{2+}+Mg)$ and Mg content all of the samples (dome and dykes) is approximately 0.5-0.3 apfu 2.9-3.8 apfu respectively.

According to the International Mineralogical Association (IMA) classification, biotite; It is divided into four end members: annite [$KFe_2+3AlSi_3O_{10}(OH)_2$], phlogopite [$KMg_3AlSi_3O_{10}(OH)_2$], siderophyllite [$KFe_22Al(Al_2Si_2)O_{10}(OH)_2$] and eastonite [$KMg_2Al(Al_2Si_2O_{10})(OH)_2$] (Rieder et al., 1998).

According to this, following the classification of Tröger (1982), all Çağlarca radial dykes had biotite (meroxene) composition, while the dome samples meroxene and phlogopite composition (Figure 9a). The fact that the total Al content and $Fe^{2+}/(Fe^{2+}+Mg)$ ratios in biotite are low and do not change supports the relationship with the absence of continental collision or continental contamination (Lalonde & Bernard, 1993).

It is suggested that biotites are divided into two: magmatic and hydrothermal (Jacobs & Parry, 1979; Fu, 1981). It is accepted that igneous biotites crystallize directly from silicate melt and generally have molecular ratios of Mg/Fe <1.0, while hydrothermal biotites have Mg/Fe >1.5 [65]. Similarly, Fu [66] reported in his study that magmatic biotites have high titanium (TiO_2 >3%) and low aluminum content (Al_2O_3 <15%), while neoform biotites have low titanium (TiO_2 <3% and mostly <2%) and high aluminum (Al_2O_3 >15%) content.

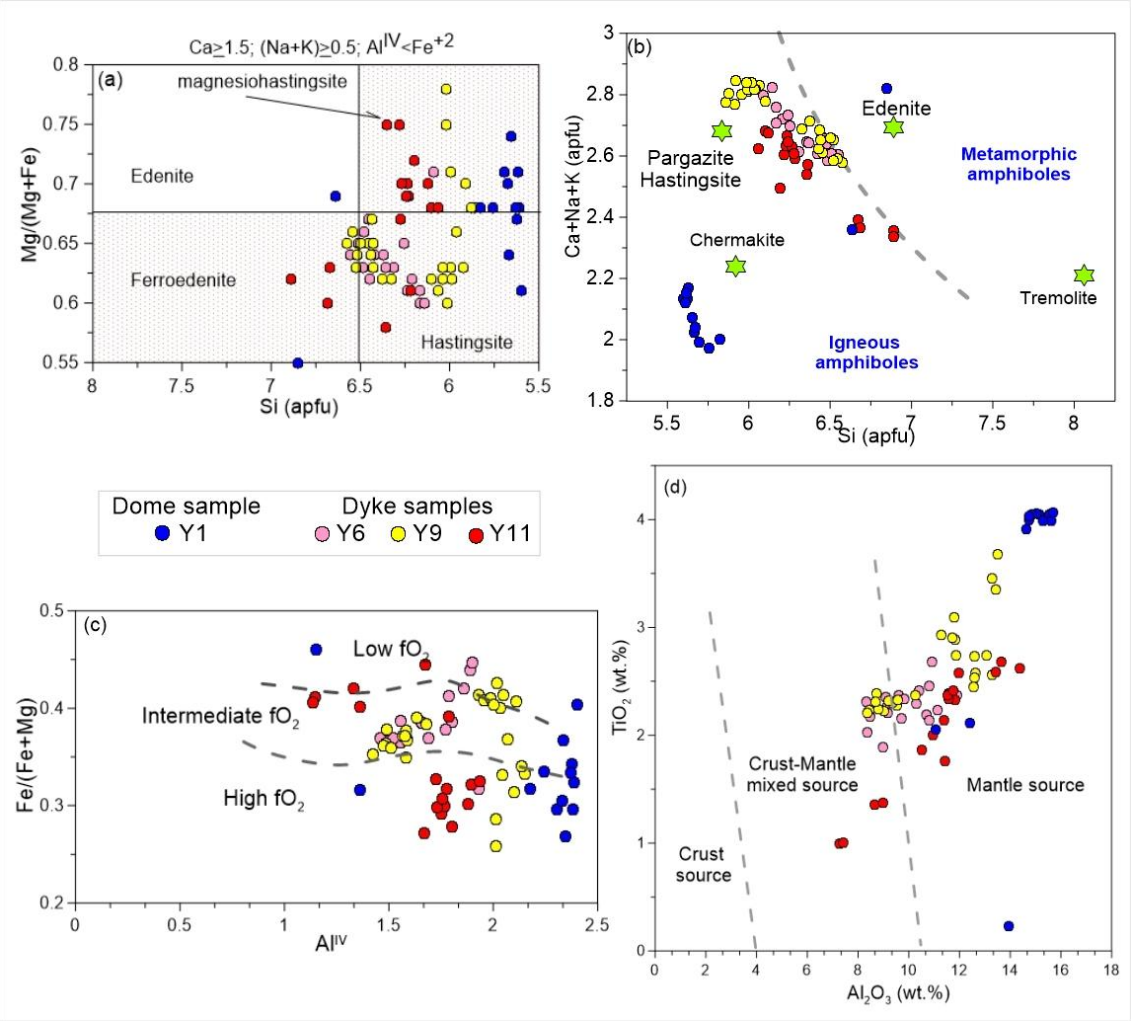

Figure 8. a) *Plots of amphibole classification diagram (Leake et al., 1997),* ***b)*** *Discrimination of magmatic and metamorphic amphibole according to Si vs. (Ca+Na+K) diagram of the Ulukale porphyritic dome and Çağlarca radial dyke samples,* ***c)*** *Al^{IV} vs. Fe/(Fe+Mg) diagram (Anderson & Smith,1995) showing the possible oxygen fugacity conditions during the crystallization,* ***d)*** *TiO_2 vs. Al_2O_3 magma source diagram for amphiboles (Jiang & An, 1984)*

Accordingly, while the biotites subject to study are compatible with neoform biotites with Mg/Fe ratios varying between 1.4-2.5 they have the characteristics of magmatic biotite in terms of TiO_2 (>3% in all samples) and Al_2O_3 (dykes <15, dome samples generally <15) contents. In the FeO+MnO-MgO-10TiO_2 triangle diagram of biotites (Nachit et al., 1985), it is seen that they are primary and re-equilibrated primary biotites (Şekil 9b). Biotites were not affected by evolution or late-stage low-temperature hydrothermal fluids (secondary crystallization). The FeO/(FeO+MgO) vs. MgO diagram suggests that all of the dykes samples and dome-Y6 sample were derived from crust-mantle mixed source while dome-Y1 sample was derived from mantle source (Figure 9c).

The Ti concentration in biotite depends on the crystallization temperature and oxygen fugacity (fO2) of biotite (Henry et al., 2005). Accordingly, low Ti content is associated with low crystallization temperature (Henry et al., 2005). According to Robert (1976) definition, the Ti content of biotite in primary magmas is generally high compared to re-equilibrated/hydrothermal/neo-formed and late-stage crystallizing magmas.

For this purpose, the Ti contents of our samples (dome and dykes 0.61-0.41) were compared with the Ti contents (0.24-0.15) of hydrothermal biotites (Tang et al., 2019). In the diagram created according to Ti, Mg and Fe contents to determine the formation temperatures of biotite (Deniz, 2022), it is seen that biotite has a pressure of 4-6 kbar and a crystallization temperature of 700-800^{0}C (Figure 9d).

Biotite chemistry is considered to be important in elucidating the petrogenesis of rocks. For this purpose, in the diagram created according to MgO--Al_2O_3 contents [61], the samples are concentrated in the orogenic magma area with calc-alkaline characteristics (Figure 9e).

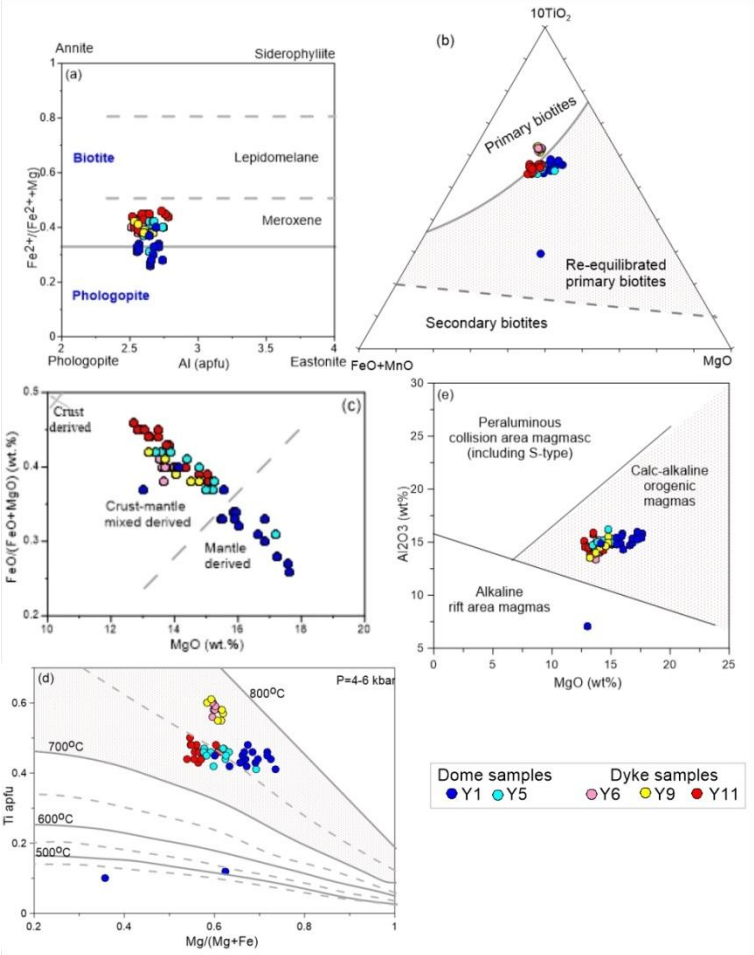

Figure 9. *Diagrams commenting biotites belonging to the Ulukale dome and Çağlarca dykes.* ***a)*** *Nomenclature of biotite in the $Fe^{2+}/(Fe^{2+}+Mg)$ vs. Al (apfu) diagram* ***b)*** *FeO+MnO-10xTiO_2–MgO triangular diagram (Nachit et al., 1985),* ***c)*** *Plots of FeO/FeO+MgO) vs. MgO for biotite (Zhou, 1986),* ***d)*** *Sample distribution in the temperature isotherm (°C) diagram calculated according to Ti and Mg/(Mg+Fe) (Tang et al., 2019),* ***e)*** *Plots of biotite composition in the MgO vs. Al_2O_3 diagram (Abdel-Rahman, 1994)*

6. CONCLUSION

This study was conducted within the Late Miocene aged Tunceli Volcanics (Karabakır Formation), -with a dome with a height of approximately 300 m and a perimeter of 4800m- and reveals the petrography and mineral chemistry characteristics of dykes (seven) of different lengths, extending from a center at different angles to form a radial shape.

Petrographic investigations identified that rocks forming the dome had basic mineral composition of plagioclase and biotite with lower amounts of amphibole, quartz and sanidine, while the basic mineral composition of the dykes was plagioclase, amphibole and sanidine with lower amounts of biotite and quartz. Among the dome and dykes with porphyritic texture and trachyandesite composition, the rocks forming the dome have larger mineral sizes and more intense alteration than the dykes. Melting-dissolution structures in plagioclase and the presence of blade-shaped biotite minerals in dykes are petrographic features that indicate magma mixing.

Plagioclase belonging to porphyritic domes and dykes is in the composition of oligoclase and andesine. The compositional similarity of plagioclase in dome and dykes is also the same in the relationships between elements. Such distributions among the elements indicate the fractionation in plagioclase.

In the chemical analysis of two pyroxene minerals found only in dykes, pyroxenes are in the composition of augite and hypersthene (two samples). Element distributions are generally consistent (except for two examples). This compositional difference is caused by the presence of hypersthene mineral as an inclusion in the augite mineral. While hypersthene with more basic composition has high Al and Ti content, samples with augite composition contain lower Al and Ti. These pyroxenes, which have calc-alkaline properties, were affected by the equilibrium crystallization conditions that enable them to crystallize under low pressure conditions (upper crust + surface conditions).

The amphiboles are mainly composed of hastingsite and magnesiohastingsite. These minerals, which originate from the mantle and feature magmatic amphibole, have different oxygen fugacity (low-medium-high). Dome samples have characteristics with a more basic composition than dyke samples.

While biotites are meroxene in composition in dykes, they are phlogopite in dome samples. Element changes/contents in biotites indicate that these minerals are of magmatic origin and primary - re-equilibrated primary biotites. Although dome and dyke samples are generally similar in terms of element distribution, dome sample Y1 points to the mantle source area, while other samples point to a crust-mantle mixture. These biotites, which feature calc-alkaline orogenic magma, were formed in the temperature range of 700-800^{o}C.

In conclusion; while one of the two dome analysis indicates a more basic composition and mantle source, while plagioclase, amphibole, and biotite minerals in and other dome and dykes specimens show generally similar properties. The elemental contents of these minerals indicate that these rocks are of magmatic origin and have not been affected by metamorphism. The fact that pyroxene mineral analysis was performed on only dyke samples makes it difficult to fully compare the domes and dykes in terms of this mineral and, accordingly, to interpret whether the magma forming the dome and dykes are the same/different. However, when all data are taken into account, the mantle-derived magma that started to form the dome, and later completed the development of both the dome and the dykes with the mantle and crust+mantle interaction. The formation of mantle+crust magma and temperature changes in biotite minerals (700-800^{0}C) resulting

from these data can be considered as indicators of post-collision crustal thickening in the Eastern Anatolia Region.

AUTHOR CONTRIBUTIONS

Conceptualization, S.K, A.S and M.Y.Y.; project management, S.K.; fieldwork, S.K and M.Y.Y.; title, S.K. and A.S.; laboratory work, A.S and M.Y.Y.; formal analysis, S.K.; data curation, S.K. and A.S.; manuscript-original draft, S.K.; manuscript-review and editing, S.K.; visualization, S.K, A.S and M.Y.Y.; All authors have read and legally accepted the final version of the article published in the journal." Authorship should be limited to those who contributed significantly to the article.

ACKNOWLEDGEMENT

The authors would like to thank the Firat University Scientific Research Projects Unit (FÜBAP) for research support (Project number FÜBAP-MF.20.22).

CONFLICT OF INTEREST

The authors declare that they have no conflicts of interest.

REFERENCES

Abdel-Rahman, A.F.M. (1994). Nature of Biotites from Alkaline, Calc-Alkaline, and Peraluminous Magmas. *Journal of Petrology*, 35(2), 525-541. https://doi.org/10.1093/petrology/35.2.525

Agostini, S., Savaşçın, M.Y., Di Giuseppe, P., Di Stefano, F., & et al. (2019). Neogene volcanism in Elazig-Tunceli area (eastern Anatolia): geochronological and petrological constraints. *Ital. Jour. Geosci.,* vol. 138, 435-455. https://doi.org/10.3301/IJG.2019.18

Anderson, J. L., &, Smith, D. R. (1995). The Effects of Temperature and fO2 on the Al-in Hornblende Barometer. *American Mineralogist*, 80, 549-559.

Arger, J., Mitchel, J., & Westaway, R.W.C. (2000). Neogene and Quaternary volcanism of southeastern Turkey. *Geological Society, London,Special Publications, 173*(1), 459-487. https://doi.org/10.1144/GSL.SP.2000.173.01.22

Atıcı, G., & Türkecan, A. (2017). Anadolu'nun volkanları, *Doğal Kay. Eko. Bült.,* 22, 1-18.

Aydın, F., Karslı, O., & Sadıklar, M.B., (2009). Compositional variations, zoning types and petrogenetic implications of low-pressure clinopyroxenes in the neogene alkaline volcanic rocks of northeastern Turkey. *Turkish J. Earth Sci.*, 18, 163-186. https://doi.org/10.3906/yer-0802-2

Aydın, F., Schmitt, A.K., Siebel, W., Sönmez, M., & et al. (2014). Quaternary bimodal volcanism in the Niğde Volcanic Complex (Cappadocia, Central Anatolia-Turkey): age, petrogenesis and geodynamic implications. *Contributions to Mineralogy and Petrology,* 168, 2-24. https://doi.org/10.1007/s00410-014-1078-3

Ball, J. L., Calder, E. S., Hubbard, B. E., & Bernstein, M. L. (2013). An assessment of hydrothermal alteration in the Santiaguito lava dome complex, Guatemala: implications for dome collapse hazards. *Bull. Volcanol.*, 75, 676. https://doi.org/10.1007/s00445-012-0676-z

Beyarslan, M., & Bingöl, A.F. (2018). Zircon U-Pb age and geochemical constraints on the origin and tectonic implications of late cretaceous intra-oceanic arc magmatics in the Southeast Anatolian Orogenic Belt (SE-Turkey). *Journal of African Earth Sciences*, 147, 477-497. https://doi.org/10.1016/j.jafrearsci.2018.07.001

Cassidy, M., Manga, M., Cashman, K., & Bachmann, O. (2018). Controls on explosive-effusive volcanic eruption styles. *Nat. Commun.*, 2839, https://doi.org/10.1038/s41467- 018-05293-3

Deer, W.A., Howie, R.A., & Zussman, J. (1992). An introduction to the rock forming minerals. 2nd ed. Harlow, Essex, England, New York, *Longman scientific and technical, London.*

Deniz, K., (2022). Mica Types as Indication of Magma Nature, Central Anatolia, Turkey. Acta Geologica Sinica, 96(3), 844-857. https://doi.org/10.1111/1755-6724.14670

Edmonds, M., Sides, I.R., Swanson, D.A., Werner, C., Martin, R.S., & et al. (2013). Magma storage, transport and degassing during the 2008-10 summit eruption at Kilauea volcano, Hawaii. *Geochim. Cosmochim. Acta*, 123, 284-301. https://doi.org/10.1016/j.gca.2013.05.038

Fink, J.H., & Griffiths, R.W. (1998). Morphology, eruption rates, and rheology of lava domes: Insights from laboratory models. *J. Geophys. Res.*, 103, 527-545. https://doi.org/10.1029/97JB02838

Fu, J.B. (1981). Chemical composition of biotite in porphyry copper deposits. *Geology and Prospecting*, 9, 16-19.

Henry, D.J., Guidotti, C.V., & Thomson, J.A. (2005). The Ti saturation surface for low to medium pressure metapelitic biotite: Implications for geothermometry and Ti substitution mechanism. *Amer. Mineral.*, 90, 316-328. https://doi.org/10.2138/am.2005.1498

Hibbard, M. J. (1991). Textural anatomy of twelve magma mixed granitoid systems. In: J. Didier, and B. Barbarin, (Eds.), *Enclaves and Granite Petrology. Development in Petrology*, (pp. 431-444). 6546968

Horwell, C.J., Baxter, P.J., Hillman, S.E., Calkins, J.A., & et al. (2013). Physicochemical and toxicological profiling of ash from the 2010 and 2011 eruptions of Eyjafjallajökull and Grímsvötn volcanoes, Iceland using a rapid respiratory hazard assessment protocol. *Environ. Res.*, 127, 63-73. https://doi.org/10.1016/j.envres.2013.08.011

Hu, J., Zhou, H., Peng, P.A., & Spiro, B. (2016). Seasonal variability in concentrations and fluxes of glycerol dialkyl glycerol tetraethers in Huguangyan Maar Lake, SE China: implications for the applicability of the MBT–CBT paleo temperature proxy in lacustrine settings. *Chem. Geol.*, 420, 200-212. https://doi.org/10.1016/j.chemgeo.2015.11.008

İmer, A., Richards, J.P., Creaser, R.A., & Spell, T.L. (2015). The late Oligocene Cevizlidere Cu-AuMo deposit, Tunceli Province, eastern Turkey. *Mineralium Deposita*, 50, 245-263. https://doi.org/10.1007/s00126-014-0533-4

Innocenti, F., Mazzuoli, R., Pasquar, G., Radicati Di Brozolo, F., & Villari, L. (1982). Tertiary and quaternary volcanism of the Erzurum-Kars area (Eastern Turkey): Geochronological data and geodynamic evolution. *J. Volcanol. Geotherm. Res.,* 13, 223-240. https://doi.org/10.1016/0377-0273(82)90052-X

Jacobs, D.C. & Parry, W.T. (1979). Geochemistry of biotite in the Santa Rita porphyry copper deposit, New Mexico. *Econonic Geology*, 74(4), 860-887. https://doi.org/10.2113/gsecongeo.74.4.860

Jiang, C. & An, S. (1984). On chemical characteristics of calcific amphiboles from igneous rocks and their petrogenesis significance. *Journal of Mineralogy and Petrology*, 3, 1-9.

Karaoğlu, Ö., Browning, J., Bazargan, M., & Gudmundsson, A. (2016). Numerical modelling of triple-junction tectonics at Karlıova, Eastern Turkey, with implications for regional magma transport. *Earth and Planetary Science Letters,* 452, 157-170. https://doi.org/10.1016/j.epsl.2016.07.037

Karaoğlu, O., Selçuk, A.S., & Gudmundsson, A. (2017). Tectonic controls on the Karlıova triple junction (Turkey): Implications for tectonic inversion and the initiation of volcanism. *Tectonophysics,* 694, 368-384. https://doi.org/10.1016/j.tecto.2016.11.018

Karaoğlu, Ö., Gülmez, F., Göçmengil, G., Lustrino, M., & et al. (2020). Petrological evolution of Karlıova-Varto volcanism (Eastern Turkey): Magma genesis in a transtensional triple-junction tectonic setting. *Lithos,* 364-365, 105524. https://doi.org/10.1016/j.lithos.2020.105524

Karslı, O., Chen, B., Uysal, I., Aydın, F., Wijbrans, J.R., & Kandemir, R. (2008). Elemental and Sr-Nd-Pb isotopic geochemistry of the most recent Quaternary volcanism in the Erzincan Basin, eastern Turkey: framework for the evalution of basalt-lower crustinteraction. *Lithos,* 106, 55-70. https://doi.org/10.1016/j.lithos.2008.06.008

Kaygusuz, A. (2009). K/Ar Ages and geochemistry of the collision related volcanic rocks in the Ilıca (Erzurum) area, eastern Turkey, *Neues Jahrbuch für Mineralogie,* 186, 21-36. https://doi.org/10.1127/0077-7757/2009/0134

Kaygusuz, A., Aslan, Z., Aydınçakır, E., Yücel, C., Gücer, M.A., & Şen, C. (2018). Geochemical and Sr-Nd-Pb isotope characteristics of the Miocene to Pliocene volcanic rocks from the Kandilli (Erzurum) area, Eastern Anatolia (Turkey): Implications for magma evolution in extension-related origin. *Lithos,* 296, 332-351. https://doi.org/10.1016/j.lithos.2017.11.003

Keskin, M. (2005). Domal uplift and volcanism in a collision zone without a mantle plume: Evidence from Eastern Anatolia. URL

Keskin, M., Pearce, J.A., & Mitchell, J. (1998). Volcano-stratigraphy and geochemistry of collision-related volcanism on the Erzurum–Kars Plateau, northeastern Turkey. *Journal of Volcanology and Geothermal Research,* 85, 355-404. https://doi.org/10.1016/S0377-0273(98)00063-8

Kocaarslan, A., & Ersoy, E.Y. (2018). Petrologic evolution of Miocene-Pliocene mafic volcanism in the Kangal and Gürün basins (Sivas-Malatya), central east Anatolia: evidence for Miocene anorogenic magmas contaminated by continental crust. *Lithos,* 310-311, 392-408. https://doi.org/10.1016/j.lithos.2018.04.021

Kuşçu, İ., Kuşçu, G.G., Tosdal, R., & Andrew, C.J. (2007). *Tectonomagmatic-metallogenic framework of mineralization events in the southern NeoTethyan arc, southeastern Turkey*. Digging Deeper. Proceedings of the 9th Biennial SGA Meeting, Dublin, (pp. 20-23).

Kürkçüoğlu, B., Pickard, M., Şen, P., Hanan, B.B., Sayit, K. & et al. (2015). Geochemistry of mafic lavas from Sivas, Turkey and the evolution of Anatolian lithosphere. *Lithos,* 232, 229-241. https://doi.org/10.1016/j.lithos.2015.07.006Get rights and content

Kürüm, S. (2011). K-Ar age, geochemical, and Sr-Pb isotopic compositions of Keban magmatics, Elazıg, Eastern Anatolia, Turkey. *National Sci.,* 3(9), 750-767. https://doi.org/10.4236/ns.2011.39100

Kürüm, S., & Baykara, T. (2020). Geochemistry of Post-Collisional Yolçatı (Bingöl) Volcanic Rocks in Eastern Anatolia, Turkey. *African Earth Sciences,* 161, 103-153. https://doi.org/10.1016/j.jafrearsci.2019.103653

Kürüm, S., Önal, A., Boztuğ, D., Spell, T., & Arslan, M. (2008). 40Ar/39Ar age and geochemistry of the post-collisional Miocene Yamadağ volcanics in the Arapkir area (Malatya Province), eastern Anatolia, Turkey. *Journal of Asian Earth Sciences,* 33, 229-251. https://doi.org/10.1016/j.jseaes.2007.12.001

Kürüm S., Akgül B., Önal A.Ö., Boztuğ D., Harlavan Y., & Ural M. (2011). An Example for Arc-Type Granitoids along Collisional Zones: The Pertek Granitoid, Taurus Orogenic Belt, Turkey. *International Journal of Geosciences,* 2, 214-226. ISSN Online: 2156-8367

Kürüm, S., Sar, A., Yurt, M.Y., & Yıldırım, İ. (2024). Petrological Features of Neogene Ulukale Porphyritic Dome and Çağlarca Radial Dykes in the Tunceli Volcanic, Eastern Turkey. *Doklady Earth Sciences,* 518(2), 1665-1678. ISSN 1028-334X.

Lalonde, A.E., & Bernard, P. (1993). Composition and colour of biotite from granites: two useful properties in the characterization of plutonic suites from the Hepburn internal zone of the Wopmay orogen, Northwest Territories. *Canadian Mineralogist*, 31, 203-217.

Leake, B.E. (1971). On aluminous and edenitic amphiboles. Mineralogical Magazine 38, 389-407. https://doi.org/10.1180/minmag.1971.038.296.01

Leake, B.E., Woolley, A.R., Arps, C.E.S., Birch, W.D., Gilbert, M.C., & et al. (1997). Nomenclature of amphiboles Report of the Subcommittee on Amphiboles of the International Mineralogical Association Commission on New Minerals and Mineral Names. *European Journal of Mineralogy*, 9, 623-651. https://doi.org/10.1127/ejm/9/3/0623

Lebedev, V., Sharkov, E., Ünal, E., & Keskin, M. (2016). Late Pleistocene Tendürek Volcano (Eastern Anatolia, Turkey): I. Geochronology and petrographic characteristics of igneous rocks. *Petrology*, 24, 127-152. https://doi.org/10.1134/s0869591116030048

Leterrier, J., Maury, R.C., Thonon, P., Girard, D., & Marchal, M. (1982). Clinopyroxene composition as a method of identification of the magmatic affinities of paleo-volcanic series. *Earth and Planetary Science Letters,* 59, 139-154. https://doi.org/10.1016/0012-821X(82)90122-4

Lin, Y.C., Chung, S.L., Bingöl, A.F., Beyarslan, M., & Lee, H.Y. (2015). *Petrogenesis of late Cretaceous Elazıg magmatic rocks from SE Turkey: New age and geochemical and Sr-Nd-Hf isotopic constraints.* Goldschmidt, 16-21 August Prag, Abstracts, 1869

Lustrino, M., Keskin, M., Mattioli, M., Lebedev, V.A., & Chugaev, A. (2010). Early activity of the largest Cenozoic shield volcano in the circum-Mediterranean area: Mt. Karacadağ, SE Turkey. *European Journal of Mineralogy*, 22, 343-362. https://doi.org/10.1127/0935-1221/2010/0022-2024

Morimoto N., Fabries J., Ferguson A.K., Ginzburg I.V., Ross M., & et al. (1988). Nomenclature of pyroxenes. *Mineralogy and Petrology*, 39, 55-76.

MTA. (2002). Geological map of Turkey. 1:500,000. *MTA*, Ankara, Turkey

Nachit, H., Razafimahefa, N., Stussi, J.M., & Caron, J.P. (1985). Composition chimique des Biotites et typologie magmatique des granitoids. C.R. Acadomic Sciences Paris, Series 2, 301, 813-818. INIST identifier 9284353

Nekvasil, H., Dondolini, A., Horn, J., Filiberto, J., Long, H., & Lindsley, D.H. (2004). The origin and evolution of silica-saturated alkalic suites: an experimental study. *Journal of Petro.* 45, 693-721. https://doi.org/10.1093/petrology/egg103

Oyan, V., Keskin, M., Lebedev, V.A., Chugaev, A.V., & Sharkov, E.V. (2016). Magmatic evolution of the Early Pliocene Etrüsk stratovolcano, eastern Anatolian collision zone, Turkey. *Lithos,* 256, 88-108. https://doi.org/10.1016/j.lithos.2016.03.017

Oyan, V., Keskin, M., Lebedev, V.A., Chugaev, A.V., Sharkov, E.V., & Ünal, E. (2017). Petrology and Geochemistry of the Quaternary Mafi c Volcanism in the northeast of Lake Van, Eastern Anatolian Collision Zone, Turkey. *Journal of Petrology,* 58, 1701-1728. https://doi.org/10.1093/petrology/egx070

Önal, A., Boztuğ, D., Arslan, M., Spell, T.L., & Kürüm, S. (2008). Petrology and 40Ar-39Ar age of the bimodal Orduzu Volcanics (Malatya) from the western end of the eastern Anatolian Neogene volcanism, Turkey. *Turkish Journal of Earth Sci.,* 17, 85-109. https://journals.tubitak.gov.tr/earth/vol17/iss1/4

Özdemir, Y., Karaoğlu, Ö., Tolluoğlu, A.Ü., & Güleç, N. (2006). Volcanostratigraphy and petrogenesis of the Nemrut stratovolcano (East Anatolian high plateau): the most recent post-collisional volcanism in Turkey. *Chemical Geology*, 226, 189-211. https://doi.org/10.1016/j.chemgeo.2005.09.020

Pearce, J., Bender, J., De Long, S., Kidd, W., Low, P., & et al. (1990). Genesis of collision volcanism in Eastern Anatolia, Turkey. *Journal of Volcanology and Geothermal Research*, 44, 189-229. https://doi.org/10.1016/0377-0273(90)90018-B

Rabayrol, F., Hart, C.J.R., & Thorkelson, D.J. (2019). Temporal, spatial and geochemical evolution of late Cenozoic post-subduction magmatism in central and eastern Anatolia, Turkey. *Lithos,* 336(337), 67-96. https://doi.org/10.1016/j.lithos.2019.03.022

Rieder, M., Cavazzini, G., D´Yakonov, Y.S., Frankkamenetskii, V.A., Gottardi, G., & et al. (1998). Nomenclature of the mica. Canadian Mineralogist 36, 905-912.

Robert, J.L. (1976). Titanium solubility in synthetic phlogopite solid solutions. Chemical Geology, 17(3): 213-227.

Rosas-Carbajal, M., Komorowski, J.C. Nicollin, F., & Gibert, D. (2016). Volcano electrical tomography unveils edifice collapse hazard linked to hydrothermal system structure and dynamics, *Sci. Rep.*, 6, 29899.

Sar, A., Ertürk, M.A., & Rizeli, M.E. (2019). Genesis of Late Cretaceous intra-oceanic arc intrusions in the Pertek area of Tunceli Province, eastern Turkey, and implications for the geodynamic evolution of the southern Neo-Tethys: Results of zircon U–Pb geochronology and geochemical and Sr-Nd isotopic analyses, *Lithos,* 105263, 350-351. https://doi.org/10.1016/j.lithos.2019.105263

Sar, A., Rizeli, M.E., & Ertürk, M.A. (2022). Petrographic and Geochemical Characteristics of the Rocks Belonging to the Elazıg Magmatic Complex in the Geçityaka region (Tunceli). *El-Cezerî Journal of Science and Engineering,* 9(2), 680-694. https://doi.org/10.31202/ecjse.993333

Tang, P., Yuchuan, Y.,, Tang, J., Wang, Y., Zheng, W., & et al. (2019). Advances in research of mineral chemistry of magmatic and hydrothermal biotites. *Acta Geologica Sinica,* 93(6), 1947-1966. https://doi.org/10.1111/1755-6724.14395

Tröger, W.E. (1982). *Optische Bestimmung der gesteinsbildenden Minerale, Teil 2.* Scheweizerbartsche Verlagsbuchhandlung, Stuttgart. (pp.822)

Turner, M., Turner, S., Mironov, N., Portnyagin, M., & Hoernle, K. (2017). Can magmatic water contents be estimated from clinopyroxene phenocrysts in some lavas? A case study with implications for the origin of the Azores Islands. *Chem Geol.,* 466, 436-445. https://doi.org/10.1016/j.chemgeo.2017.06.032

Xu, W., Zhao, Z., & Daı, L. (2020). Post-collisional mafic magmatism: Record of lithospheric mantle evolution in continental orogenic belt. *Science China Earth Sciences,* 63, 2029-2041. https://doi.org/10.1007/s11430-019-9611-9

Yılmaz, Y., Güner, Y., & Şaroğlu, F. (1998). Geology of the quaternary volcanic centres of the east Anatolia. *Journal of Volc. and Geoth. Research,* 85, 173-210. https://doi.org/10.1016/S0377-0273(98)00055-9

Zhang, J.Q., Li, S.R., Santosh, M., Wang, J-Z., & Li, Q. (2015). Mineral chemistry of high-Mg diorites and skarn in the Han-Xing Iron deposits of South Taihang Mountains, China: Constraints on mineralization process, *Ore Geology Reviews,* 64, 200-214. https://doi.org/10.1016/j.oregeorev.2014.07.007

Zhou, Z.X. (1986). The origin of intrusive mass in Fengshandong, Hubei province. *Acta Petrol. Sin.,* 2 (1), 59-70 (in Chinese with English abstract).